Translational Oncology 13 (2020) 100854

Contents lists available at ScienceDirect

Translational Oncology

journal homepage: www.elsevier.com/locate/tranon

Synthesis of ^{99m}Tc-labeled 2-Mercaptobenzimidazole as a novel radiotracer to diagnose tumor hypoxia

Syed Faheem Askari Rizvi [a,b], Haixia Zhang [a,*], Sajid Mehmood [b], Mahmoud Sanad [c]

[a] College of Chemistry and Chemical Engineering, Lanzhou University, Lanzhou 730000, Gansu, PR China
[b] Isotope Production Group, Chemistry Division, Pakistan Institute of Nuclear Science and Technology (PINSTECH), P.O. Nilore, Islamabad, Punjab, Pakistan
[c] Labeled Compounds Department, Hot Laboratories Center, Atomic Energy Authority, P.O. Box 13759, Cairo, Egypt

ARTICLE INFO

Article history:
Received 28 May 2020
Received in revised form 24 July 2020
Accepted 3 August 2020
Available online xxxx

Keywords:
Imidazole
Radiotracer
Tumor hypoxia
^{99m}Tc-2-MBI
Scintigraphy study
S180 Tumor

ABSTRACT

Discovery of ^{99m}Tc-labeled imidazole derivatives as a potential radiotracer for hypoxic tumor imaging is considered to be of great interest because of non-invasive detection capabilities. 2-Mercaptobenzimidazole (2-MBI) was successfully synthesized, characterized and radiolabeled with $[^{99m}Tc(CO)_3(H_2O)_3]^+$ intermediate to form ^{99m}Tc-2-MBI complex with radiochemical purity of ≥ 95% yield as observed by instant-thin layer chromatography (ITLC) and radio-high performance liquid chromatography (radio-HPLC). The ^{99m}Tc-2-MBI complex was observed to be stable in saline and serum with no noticeable decomposition at room temperature and 37 °C, respectively, over a time period of 24 h. Biodistribution results in Balb/c mice bearing S180 tumor show that ^{99m}Tc-2-MBI highly internalized in tumor tissue, also possess preferably high tumor/muscle and tumor/blood ratios 4.14 ± 0.77 and 3.91 ± 0.63, respectively at 24 h incubation. Scintigraphic imaging study shows ^{99m}Tc-2-MBI is visibly accumulated in hypoxic tumor tissue, suggesting it would be a promising radiotracer for early stage diagnosis of tumor hypoxia.

Introduction

The single benzene ring incorporated with five member imidazole is referred to as 1*H*-benzimidazole or 1,3-benzodiazole. Benzimidazole and its derivatives have wide applications as therapeutic agent such as anthelmintic and antiulcer drugs. Except this, they also display pharmacological activities including anticancer, antimicrobial, antitubercular, analgesic, and antiviral and many more [1–3]. Imidazole or iminazoline contains an azapyrrole moiety having two nitrogen atoms separated by one carbon atom. This compound was first prepared in 1958 by reacting glyoxal with ammonia, thus also called as glyoxalin [4,5]. Common examples of such biomolecules containing benzimidazole as basic subunit are Guanine, adenine, purine, caffeine and uric acid [6,7]. Literature provides ample knowledge on versatile methods for synthesis of various homo- and hetero-, mono- and di-substituted derivatives of benzimidazole with biological and clinical applications [8–15]. A series of benzoimidazole derivatives have also been synthesized which depict anticancer activities against various types of solid tumor. The synthesized compounds were further tested for their in vitro antiproliferative activities and reported non-specific antiproliferative effect on tested cell lines [16]. Sondhi et al., 2010 reported the synthesis of heterocyclic benzimidazole derivatives and evaluated their potential for anticancer activity against ovary, breast and CNS human cancer cell lines [17]. Zhang el al., 2006 synthesized radiolabeled nitro-benzimidazole and nitrotriazole derivatives and studied their potential to diagnose tumor hypoxia [18]. Alberto 2005 elaborated the coordination chemistry of monodentate and bidentate imidazole ligands with ^{99m}Tc-tricaronyl precursor and also highlighted x-ray studies to support the structural outcomes [19]. Furthermore, Li et al., 2015 and Ruan et al., 2018 also synthesized technetium-99 m labeled 4-nitroimidazole dithiocarbamate and isocyanide derivatives, respectively as potential agents for tumor hypoxia [20,21]. Experimental outcomes provide fruitful evidences on utilization of benzimidazole derivatives as potential agents for targeting tumor hypoxia [22–25].

Many human pathological processes underwent low concentration of oxygen (hypoxia) including stroke, ischaemic heart disease and cancer. Hypoxia or oxygen deprivation is a root factor in tumor progression and therapeutic resistance because of its devastating effect on molecular genetics, metabolic and pathophysiologic adaptive processes such as neoangiogenesis. Hypoxia in solid tumors is mainly due to imbalance delivery of oxygenated blood to overcome increased metabolic demand of promptly proliferating tumor cells [26,27]. The prevalence of hypoxic areas is a characteristic feature of solid tumors and human malignancies such as cancer of uterine cervix, breast, valve, prostate, head and neck, pancreas, rectum as well as brain carcinoma, malignant melanomas and soft tissue sarcomas [28]. Non-invasive detection of tumor hypoxia can predict treatment strategy and provide aid in order to support treatment decisions. Such non-invasive imaging modalities are widely available in clinical

* Corresponding author.
E-mail address: Zhanghx@lzu.edu.cn. (H. Zhang).

http://dx.doi.org/10.1016/j.tranon.2020.100854

practice including oxygen electrodes, blood-oxygen level dependent (BOLD) and tissue-oxygen level dependent (TOLD) based magnetic resonance imaging (MRI), positron emission tomography (PET) and single photon emission computed tomography (SPECT). PET/SPECT imaging quantify data at macroscopic level in tumor tissue and displays advantages over other imaging techniques for treating hypoxia, as they utilize radiotracer probes, which can directly measure oxygen level and permit non-invasive detection of intra-tumor oxygen level instead of hypoxia-mediated transformations in phenotype [26,29]. Alberto et al. 1998 first reported the preparation of $[^{99m}Tc(CO)_3(H_2O)_3]^+$ precursor from sodium pertechnetate, which has attracted great attention globally as it can be easily synthesized and readily substituted water molecules through various functional groups, also possessing small size and inertness [30]. So far, ^{99m}Tc-tricarbonyl precursor has been successfully used for radiolabeling of various biologically active molecules with variety of ligands [31,32].

Keeping in mind the importance and benefits associated with usefulness of derivatives of benzimidazole, the aim of our study is to synthesize 2-Mercaptobenzimidazole (2-MBI) and radiolabel it with $[^{99m}Tc(CO)_3(H_2O)_3]^+$ to yield ^{99m}Tc-2-MBI and evaluate its potential to target tumor hypoxia. Analytical characterization methods were used to investigate and confirm the formation of ^{99m}Tc-labeled complex. In vitro and in vivo biological evaluation studies were carried out in order to interrogate the effective of radiopharmaceutical to diagnose tumor hypoxia.

Materials and methods

Chemicals and reagents

O-phenylenediamine, carbon disulfide, potassium hydroxide, sodium hydroxide, stannous chloride dihydrate and all necessary chemicals were purchased from sigma-aldrich, Germany. All reagents including ethanol, dimethyl sulfoxide (DMSO), DMSO-D_6, methanol, acetone, hydrochloric acid (HCl), and acetonitrile were of analytical grade, used without further purification and purchased from Merck, Germany. Whatman paper No. 3 and instant thin-layer chromatography impregnated with silica gel (ITLC-SG) were bought from Agilent, Singapore. pH paper of Merck, Germany was used to adjust pH of all standard/ stock solutions used in this study. Technetium-99 m was eluted in the form of sodium pertechnetate ($^{99m}TcO_4^-Na^+$) using 0.9% saline from locally produced ^{99}Mo/^{99m}Tc generator PAKGEN at Pakistan Institute of Nuclear Science and Technology (PINSTECH), Nilore, Islamabad-Pakistan.

Equipments

All instruments used in this study were properly calibrated and validated by Mechanical Division of the institute. All kind of standard glassware used in this study was properly sterilized using Autoclave (Make-Indfos) at 121 °C for 20 min. To scan the chromatographic strips, 2π-Scanner (Berthold, Germany) was used. Characterization studies were performed using Deluxe Electrophoresis Chamber (Gelman, Germany) system, D-200 Elite HPLC system interconnected with C-18 column 4.6 × 150 mm (Inertsil® ODS-3, GL Sciences) along with NaI(Tl) detector, NMR spectra was recorded using ECS 400 MHz instruments (JEOL Resonance, Japan). ^{1}H NMR chemical shifts (δ) were recorded relative to DMSO-D_6 (δ = 2.50 ppm). High-resolution mass spectroscopy was performed on ORBITRAP ELITE (Thermo Scientific). Scintigraphy study was performed using Dual-headed Siemens Integrated Gamma Camera (interfaced with high-resolution parallel hole collimator) while blood cell images were captured using LED microscope (Zeiss Primo Star).

Chemistry

Synthesis of 2-Mercaptobenzimidazole

For the synthesis of 2-Mercaptobenzimidazole (2-MBI), the synthesis protocol reported by Al-Mohammed et al., 2013 was followed after necessary modifications [10]. Briefly, potassium hydroxide (Mr. 59, 1.9 g; 0.03 mol) was dissolved in a mixture of 30 mL ethanol (60%) and 20 mL water (40%). Next, carbon disulfide (Mr. 76, 2.69 g; 0.03 mol) was added with stirring and mixture was allowed to boil at 80 °C. After that, *o*-phenylenediamine (Mr. 108, 3.45 g; 0.03 mol) was dissolved in 20 mL ethanol at room temperature and added dropwise into the mixture of KOH/CS_2 and allowed to reflux it for 6 h at 75–85 °C. Upon completion of reaction (monitored via TLC), the ethanol was removed and white residue was dissolved in water and precipitated using 50% dilute acetic acid. The product was then recrystallized by using a mixture of water-ethanol (1:1) to get 2-Mercaptobenzimidazole (Mr. 150, 4.5 g; 0.045 mol) in 74% yield, M.P. 258 °C (Lit. 255–256 [33]). Ultra-high pressure liquid chromatography (UHPLC) gives ≥97% purity of product with peak at R_t = 5.007 min (see ESI, Fig. S1) using a mixture of acetonitrile and sodium phosphate buffer pH 7.4 (50,50 *v*/v) at 255 nm. ^{1}H NMR (400 MHz, DMSO-D_6, see ESI, Fig. **S2**): δ 12.4 (s, 1H, -SH), 7.54 (d, J = 2H, ArH), 7.53 (d, J = 2H, ArH), 7.06 (d, J = 1H, -NH). HRMS (ESI): m/z [M + H^+] calculated for $C_7H_6N_2S$: 151.0324, found: 151.0327 (M = 100%). The crystallinity of the final product was characterized by X-ray powder diffraction (XRPD) analysis with major peaks at position 14.84, 23.61, 28.46, 32.28 and 43.52 2(θ) degree which is similar to the spectrum reported in literature [34,35] (see ESI, Fig. S3).

Radiolabeling of ^{99m}Tc-tricarbonyl complex

The Technetium-99 m-tricarbonyl precursor was synthesized by following the procedure reported in literature [30,36]. Briefly, sodium carbonate (Na_2CO_3) 5 mg, potassium sodium tartrate 15 mg and Sodium borohydride ($NaBH_4$, as reducing agent) 10 mg were dissolved in saline (0.9% NaCl/H_2O) in a 10 mL glass vial, followed by sealing and flushing with CO for 15 min. Then, freshly eluted $^{99m}TcO_4^-$ (555 MBq/ mL saline) was added in reaction mixture and heated for 30 min at 75–80 °C. After successful synthesis of precursor $[^{99m}Tc(CO)_3(H_2O)_3]^+$, mixture was cooled and pH was adjusted to 5 using 0.1 M HCl. After that, 2-Mercaptobenzimidazole 1 mg was added, followed by heating at 95 °C for 30 min under nitrogen. The radiochemical purity of the ^{99m}Tc-labeled complex (^{99m}Tc-2-MBI) was assessed by radio-HPLC using gradient mobile phase system A: H_2O (0.1% TFA) 0–2 min 90%, 2–5 min 60%, 5–10 min 10% with B: acetonitrile (0.1% TFA) accordingly. HRMS (ESI): m/z calculated for $[^{99m}Tc(CO)_3(H_2O)]$-$C_7H_4N_2S$: 349.1410, found: 349.1042 (M = 100%).

In vitro stability study

In vitro stability assay was carried out to monitor the effective degradation potential of newly synthesized radiopharmaceutical in saline (0.9% NaCl in H_2O) and to evaluate the possible biocompatibility in mice serum by following the protocol reported by Rizvi and co-workers [37]. For saline stability analysis, 1.5 mL saline was added in 10 mL glass vial followed by addition of ^{99m}Tc-2-MBI (185 MBq/mL) and incubated for 24 h at room temperature. For serum stability assay, serum plasma was separated from freshly eluted blood of normal mice and centrifuged at 350 ×g for 5–10 min. A sterilized reaction vial containing ~0.2 mL ^{99m}Tc-2-MBI (111 MBq) was taken and about 1.8 mL serum was added, vortex shaken for 30 s and incubated for 24 h at ambient temperature. To assess the percent radiochemical purity (%RCP) of the complex at various time intervals (i.e. 0.5 h, 1 h, 4 h and 24 h), ~5 μL aliquot of sample mixture was spotted at bottom line of Whatman paper No.3 (3MM) and ITLC-SG strips (1 × 10 cm) for ascending paper chromatography. 3MM strip was hangout in acetone to monitor the reduced/free ^{99m}Tc (R_f = 1), meanwhile ITLC-SG was hangout in 1 M NaOH to monitor reduced/ hydrolyzed ^{99m}Tc (R_f = 0) in sample mixture. The strips were heat-dried and scanned with 2π-scanner (Berthold, Germany). The results were reproduced thrice (n = 3).

Electrophoresis was also performed to observe the charge nature of resulting complex using paper electrophoresis method. Whatman Paper No. 1 strip (2 × 20 cm; as supporting medium) was place in electrophoresis chamber (Deluxe Gelman, Germany) having 0.02 M sodium phosphate buffer (pH 6.8; as electrolyte). An aliquot of ~10 μL was spotted at the center of the strip and run at 300 DC volts for 45 min. Upon completion, the

strip was heat-dried and scanned on 2π-scanner (from left to right) to get required chromatogram.

Animals and cell culture

Murine sarcoma S180 cell line was obtained for in vitro study from Phytochemical Lab of Pakistan Institute of Engineering and Applied Sciences (PIEAS), Nilore, Islamabad-Pakistan. Hypoxic tumor S180 induced female Balb/c mice (~20–30 g; three mice in each set) were purchased from National Institute of Health (NIH), Islamabad, Pakistan. The animal ethical review committee of the institute (NIH) gave approval to conduct anticancer study in tumor animal models in current experiments.

Cellular uptake assay

To investigate the cellular uptake of radiopharmaceutical, S180 cell were incubated under hypoxic and aerobic conditions as protocol reported in literature [18]. S180 cells were cultured in DMEM medium containing 10%FBS with 1% penicillin/streptomycin at a concentration of 2×10^6 cells/mL medium. The cells were incubated at 37 °C under an atmosphere of hypoxic exposure (95% N_2: 5% CO_2, $O_2 < 10$ ppm) and aerobic exposure (95% Air: 5% CO_2) for 30 min with gentle shaking. After equilibration, ^{99m}Tc-2-MBI (7.4 MBq/ 0.2 mL) and drug concentration of 15 μg/mL was added in each vial and 0.5 mL suspension was subjected to centrifugation at 300 ×*g* for 5 min at various time intervals (say 0.5, 1, 2, 4, and 6 h post-incubation; >90% viable cells). The supernatant 0.4 mL was separated for counting (C_{out}) using well-type NaI γ-counter and remaining cells including 0.1 mL medium was also counted (C_{in}). The experiment was repeated thrice ($n = 3$). The final cell accumulation "A" was calculated by applying formula:

$$A = (C_{in} – C_{out}/4)/(C_{in} + C_{out})$$

Cytotoxicity study

The unusual shape of red blood cells (RBCs) or abnormal counting of cells indicates the cytotoxicity behavior of radiopharmaceuticals. To observe this cytotoxicity behavior of ^{99m}Tc-2-MBI, freshly eluted RBCs were withdrawn from cardiac puncture of mice during biodistribution study and spread on a glass slide to make uniform layer of blood cells. The slide was placed under LED microscope (Zeiss Primo Star) and shape and counts were measured for 4 h.

Biodistribution study

To investigate the possible distribution pattern of newly developed radiopharmaceutical in mice models, three sets of mice bearing S180 tumor were administered intravenous injection of ^{99m}Tc-2-MBI (74 MBq / 200 μL saline) through tail vein and dissected after chloroform anesthesia at 30 min, 4 h and 24 h post-injection. The organs including brain, heart, lungs, liver, stomach, kidneys, muscle, tumor, bladder, blood, and body were collected, washed twice with 0.9% saline, weighted and radioactivity was measured using well-type NaI detector. The organ distribution pattern was calculated as percentage of injected dose per gram (%ID/g). The results were repeated thrice ($n = 3$). All animal experiments were conducted in compliance with regulations on animal's laboratory of NIH, Islamabad-Pakistan.

Metabolic study

Furthermore, in vivo metabolic stability study was also performed for ^{99m}Tc-2-MBI. A set of three healthy Balb/c mouse were administered with ^{99m}Tc-2-MBI (74 MBq / 150 μL saline) via tail vein. At 1 h post-injection, the mice were sacrificed and urine, blood and liver samples were collected. The sampled were treated as reported in literature [36]. Briefly, the urine sample was diluted with saline (1:1 *v*/v) as collected. The blood sample (0.5 mL) was centrifuged (350 ×*g* for 5 min) immediately to separate plasma serum (0.2 mL) followed by addition of 0.3 mL of acetonitrile and precipitated protein was collected after centrifugation. The liver was washed twice with saline and homogenized in 2 mL of saline-acetonitrile mixture (1:1 v/v) using a homogenizer at high speed for 5 min. After appropriate homogenization, the mixture was centrifuged at 450 ×*g* for 5 min and supernatant was passed through 0.22 μm millipore filter. All samples were subjected to radio-HPLC using above mentioned conditions.

Scintigraphy study

For scintigraphy imaging study, a set of three Balb/c mice bearing S180 hypoxic tumor in left leg were used. The mice were placed on hard flat surface with spreading front and fore legs under dual-headed Gamma camera (Siemens Integrated and interfaced with HR-parallel hole collimator) connected with online dedicated computer. All legs were fixed with surgical tape. Intravenous injection of ^{99m}Tc-2-MBI (74 MBq / 200 μL saline) was injected through marginal tail vein and whole body acquisition (static images) was carried out at 1 h after administration.

Results

Chemistry

Synthesis of 2-MBI

The synthesis of 2-Mercaptobenzimidazole (2-MBI) was successfully achieved by reacting *o*-phenylenediamine (0.03 mol) with an equivalent amount of carbon disulfide in the presence of potassium hydroxide as catalyst [10]. The schematic illustration of chemical reaction is presented in Fig. 1(Step-I). The molecular structure of *o*-phenylenediamine containing two active amino groups responsible for making suitable reaction with carbon disulfide in KOH solution at feasible temperature range to yield the corresponding 2-Mercaptobenzimidazole product with ~74% yield. The HPLC analysis shows ≥98% purity of final product, inset figure shows white crystalline residue with expected 3D structure as presented in Fig. 2(a). The structural confirmation of 2-MBI was further evaluated by ^{1}H NMR, HRMS and XRD (see ESI; Fig. S1-S3) techniques and results obtained were in agreement with our proposed structure. Table 1 shows the d-distance and relative intensities (I/I_o) of 2-MBI which is almost similar to the results reported in literature [38,39].

Radiolabeling

The radiosynthesis of ^{99m}Tc-2-MBI was carried out by following the procedure as shown in Fig. 1 (Step-II, -III). The ^{99m}Tc-tricarbonyl complex was formed as described by Zhang et al., [18] and radiochemical purity was assessed by radio-HPLC analysis which shows peak at 8.55 min with >99% purity of the complex (see ESI; Fig. S4). 2-MBI was added with intermediate ^{99m}Tc-tricarbonyl complex to give final product which is confirmed by HRMS analysis giving peak at *m/z* calculated for $^{99m}Tc(CO)_3(H_2O)$-$C_7H_4N_2S$: 349.1035 (or termed as ^{99m}Tc-2-MBI) found: 349.1042 (M = 100%) (see ESI; Fig. S5). The water molecules in $[^{99m}Tc(CO)_3(H_2O)_3]^+$ precursor were readily substituted by sulfur and nitrogen atoms in 2-MBI ligand. The radiochemical purity (RCP) of the ^{99m}Tc-2-MBI complex was assessed by instant thin-layer chromatography (ITLC) and radio-high performance liquid chromatography (Radio-HPLC) methods. By ITLC, instant thin-layer chromatography impregnated with silica gel (ITLC-SG) strip was hangout in acetone to evaluate the free ^{99m}Tc which moved with solvent front ($R_f = 0.8–1.0$) and ^{99m}Tc-2-MBI complex remained at origin ($R_f = 0.0–0.2$). Moreover, ITLC-SG strip was hangout in 1 M NaOH with ^{99m}Tc-hydrolyzed remained at point of spotting ($R_f = 0.0–0.1$) while ^{99m}Tc-2-MBI moved with solvent front ($R_f = 0.8–0.9$) as shown in Fig. S6 (see ESI). Radio-HPLC analysis finally confirms the formation of single product ^{99m}Tc-2-MBI and free ^{99m}Tc with retention times R*t* = 6.214 min and R*t* = 2.198 min, respectively as shown in Fig. 2(b), while a minor peak at R*t* = 8.593 min indicating free precursor $[^{99m}Tc(CO)_3(H_2O)_3]^+$ was observed during radio-HPLC analysis up to 10 min run time (chromatogram not shown here). The radiochemical purity of the final complex is 96 ± 0.9% ($n = 3$), suggesting that it is suitable to use for in vitro and in vivo studies without further purification.

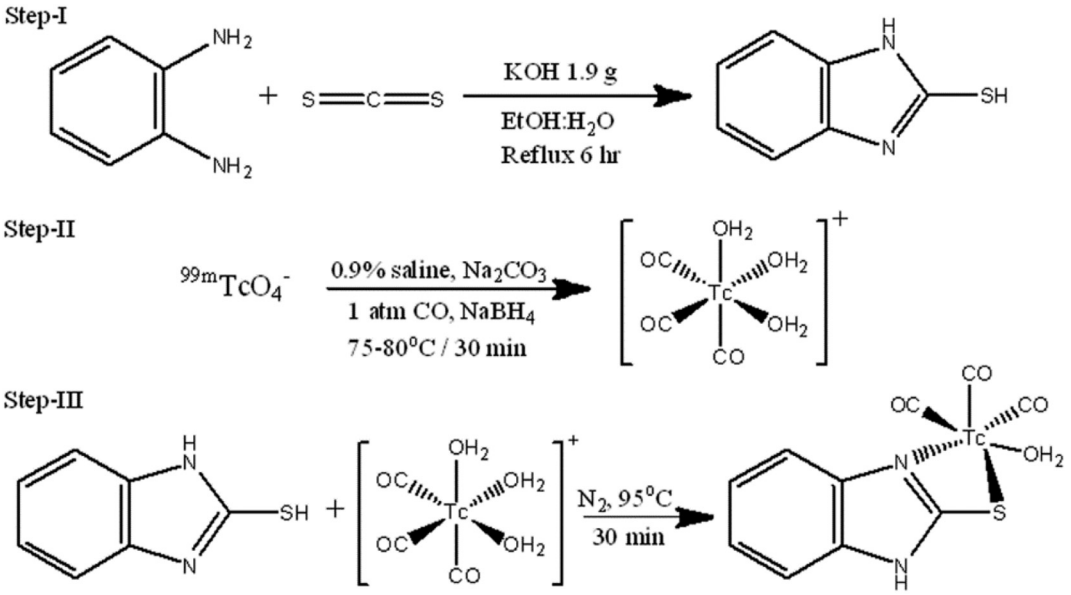

Fig. 1. (Step-I) shows formation of 2-Mercaptobenzimidazole in single step reaction. (Step-II, -III) shows formation of ^{99m}Tc-2-Mercaptobenzimidazole complex with high purity observed.

Electrophoresis and in vitro stability

The electrophoresis study presented in Fig. 3 highlights that the radiotracer has neutral nature which is more favorable to show high biocompatibility. In vitro stability study presented in Fig. 4 shows that ^{99m}Tc-2-MBI is stable in reaction mixture (0.9% saline) at room temperature up to 24 h with recorded >92% stability. At the same time, serum stability study also gives promising stability in mice serum for up to 24 h with

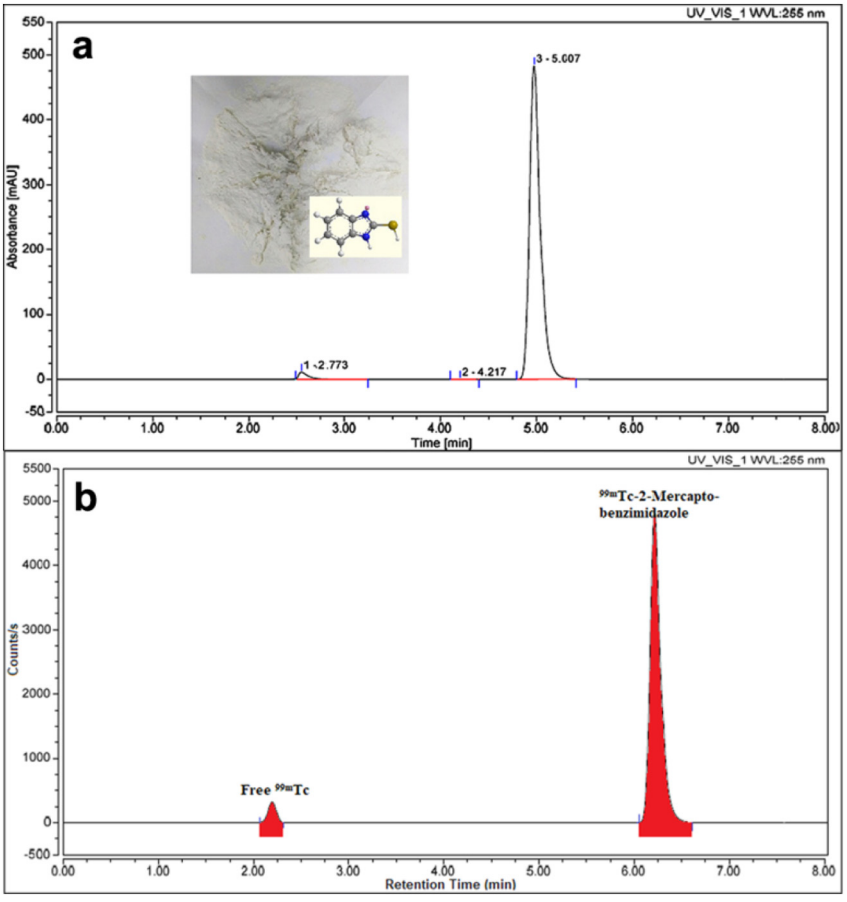

Fig. 2. The HPLC chromatograms show single peak at (a) retention time 5.007 min for pure 2-MBI, inset figure shows white crystalline powder and possible 3D-structure of 2-MBI and (b) retention time 6.214 min for ^{99m}Tc-2-MBI, suggesting that one product formed with >96% purity.

Table 1
X-ray powder diffraction data for *d*-distance and relative intensities (I/I_o) of 2-Mercaptobenzimidazole pattern.

2θ (degree)	*d* (A°)	I/I_o (%)
14.8479	5.9764	1.92
23.6114	3.7650	2.03
28.4679	3.1328	1.90
32.2811	2.7709	2.37
43.5296	2.0774	3.19

greater than 93% stability retained, suggesting ^{99m}Tc-2-MBI exhibited good in vitro stability.

Cellular uptake study

The cellular uptake potential of ^{99m}Tc-2-MBI complex in S180 cells as a function of time was carried out under hypoxic and aerobic conditions as illustrated in Fig. 5. The graph shows that the radiopharmaceutical has greater potential to accumulate in cells under hypoxic exposure than the cells incubated under aerobic condition, suggesting that ^{99m}Tc-2-MBI possess good hypoxia selectivity. Cellular uptake for hypoxic cells is significantly and persistently higher for each time point than aerobic cells ($p < 0.05$).

Biodistribution study

The biodistribution pattern of ^{99m}Tc-2-MBI was performed in S180 tumor induced Balb/c mice models (three mice for each set; $n = 3$), for each time interval i.e. 0.5 h, 4 h and 24 h the data is presented in Fig. 6a. At each time point, the radiopharmaceutical was highly accumulated in tumor tissues (11.17 ± 1.77, 12.94 ± 2.09, 9.95 ± 1.89%ID/g, respectively) in comparison with normal muscle tissues. In reference to target/non-target (T/NT) ratio, ^{99m}Tc-2-MBI showed highest tumor/muscle and tumor/blood ratios at 24 h post-injection with T/NT = 4.14 ± 0.77 and 3.91 ± 0.63, respectively, showing 38% tumor uptake (Fig. 6b), which is favorably high stability of ^{99m}Tc-2-MBI in tumor tissue. In case of normal tissues, the radiopharmaceutical ^{99m}Tc-2-MBI showed high uptake in lungs, liver and kidneys (8.21 ± 1.87, 12.63 ± 1.89 and 3.46 ± 0.63, respectively) after 24 h incubation, suggesting that the drug have metabolism through hepatobiliary pathway and excreted through urinary pathway. Furthermore, the less uptake of ^{99m}Tc-2-MBI in thyroid and stomach indicating that no $^{99m}TcO_4^-$ was found in mice after administration of ^{99m}Tc-labeled complex. To be a potential hypoxic tumor imaging agent, it is necessary to show effective tumor uptake and high tumor-to-background ratio. Also it should carry very less toxicity to normal cells and tissues. Blood samples pre- and post-injection of ^{99m}Tc-2MBI in mice models were collected on slides and investigated under inverted microscope (Zeiss Primo Star), imaging results showed normal shape and structure of blood cells with no deformation in their biconcave shape as presented in Fig. 6c. This indicates that ^{99m}Tc-2-MBI has no harmful and/or cytotoxicity effects on red blood cell counts.

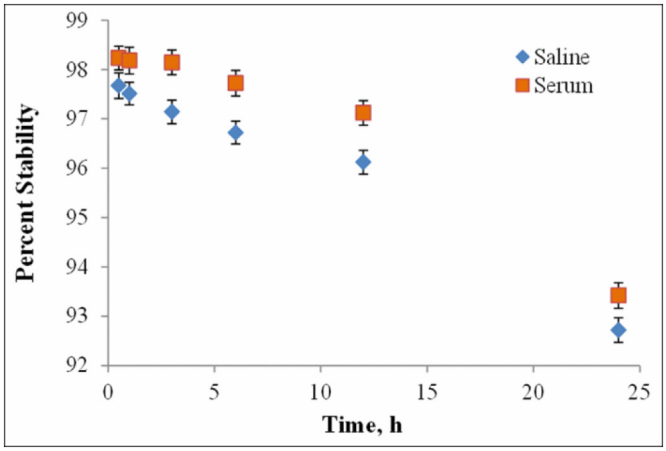

Fig. 4. In vitro stability study of ^{99m}Tc-2-MBI shows promising stability of complex in 0.9% saline and mice serum for up to 24 h.

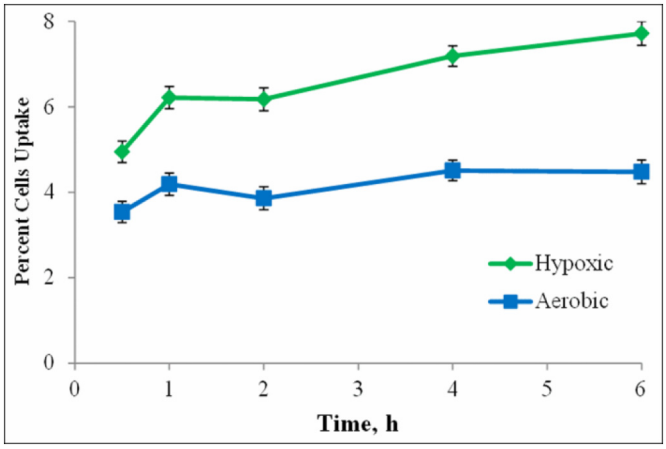

Fig. 5. Cellular uptake of ^{99m}Tc-2-MBI in S180 cells under hypoxic and aerobic conditions incubated for up to 6 h.

Metabolic stability study

The radio-HPLC analysis was further carried out for urine, blood and liver samples to investigate the metabolic stability in vivo of ^{99m}Tc-2-MBI as presented in Fig. 7. The complex remained intact in blood and urine samples (Fig. 7a, b), while in liver sample showed there was one metabolite present just after the peak of ^{99m}Tc-2-MBI in radio-HPLC chromatogram (Fig. 7c), indicating the hepatic metabolism of the radiopharmaceutical. Greater than 80% complex was recovered in urine from mice models and the complex was excreted unchanged.

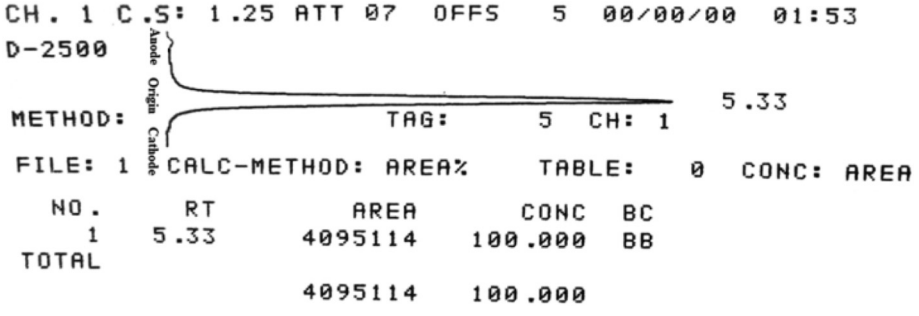

Fig. 3. The radio-chromatogram shows electrophoresis result indicating neutral nature of ^{99m}Tc-2-MBI complex as single peak observing at point of spotting, small amount of negatively charged free $^{99m}TcO_4^-$ migrate toward anode.

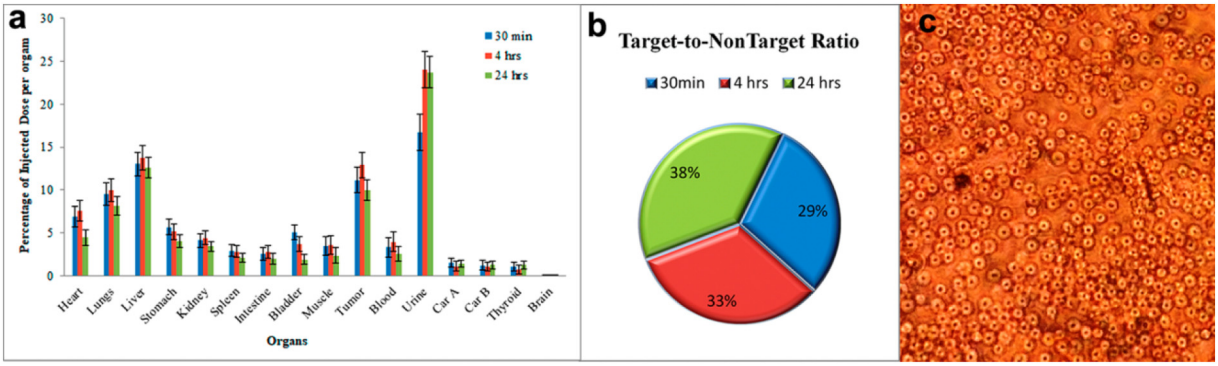

Fig. 6. In vivo S180 tumor induced mice model study illustrated (a) the possible distribution pattern of ^{99m}Tc-2-MBI in normal tissues as well as (b) shows high uptake in tumor tissue as compare to muscle tissue, while (c) cells image indicates biconcave shape of red blood cells. (For interpretation of the references to colour in this figure legend, the reader is referred to the web version of this article.)

Scintigraphy study

Scintigraphy imaging study was also performed to further investigate the hypoxic tumor imaging potential of radiopharmaceutical in Balb/c mice bearing S180 (hypoxic) tumor at 1 h post-administration of intravenous injection of 200 μL (74 MBq) of ^{99m}Tc-2-MBI. The static planar image was acquired at 1 h post-injection showed high uptake of ^{99m}Tc-2-MBI in tumor tissue, left foreleg of mice as compare to other body organs as shown in Fig. 8. The uptake in liver is due to lipophilic nature of radiopharmaceutical (log P = 1.512) while less kidney uptake and high bladder uptake was in consistent with biodistribution results and is indicating urinary excretion pathway of ^{99m}Tc-2-MBI with no free $^{99m}TcO_4^-$ detected in mice after injection. Region of interest (ROI) was drawn for getting tumor-to-normal tissue ratio as 3.39 ± 0.38 (30.2% uptake). The scintigraphy imaging results are consistent with biodistribution study results in mice, indicating that ^{99m}Tc-2-MBI successfully possess more potential as hypoxic tumor imaging agent and need further preclinical investigations.

Discussion

Tissue hypoxia has been studied in medical oncology as it plays a key role being prognostic marker concomitant with aggressive biological and clinical phenotype [40]. Regardless of its occurrence in various pathologic conditions such as stroke, myocardial ischemia and hypoxic imaging, it becoming much more advanced in oncological applications where its main role is to predict therapeutic effectiveness and also assess overall prognosis [41]. In order to diagnose tumor hypoxia, the oxygen concentration of solid tumors need to be evaluated more precisely by utilizing both invasive and non-invasive imaging techniques [42]. Imidazole functionality containing compounds have a unique property to reduce themselves into reactive intermediary metabolites through intracellular reductases (a process directly related to extend of oxygenation or hypoxia). Furthermore, these metabolites interact with thiol groups of intracellular proteins via covalent bond and then accumulate into viable hypoxic cells. However, when these compounds labeled with radiotracers, can be imaged using PET/SPECT and/or planar SPECT imaging modalities. Non-invasive techniques detect tumor hypoxia level via serial imaging, which could facilitate in gathering knowledge on disease status and treatment regime. A wide range of PET/SPECT based radiotracers including ^{123}I-IAZA, ^{99m}Tc-HMPAO, ^{99m}Tc-2-nitroimidazole, ^{99m}Tc-BRUC59–21,and ^{99m}Tc-HL-91 have been successfully synthesized and evaluated in vivo in hypoxic tumor bearing animal models as well as various types of tumor bearing patients [27–29].

In current study, we have successfully synthesized and radiolabeled novel imidazole derivative i.e. $^{99m}Tc(CO)_3(H_2O)$-2-Mercaptobenzimidazole by using a simple, facile and reproducible method. The $[^{99m}Tc(CO)_3]^+$ core being soft receptor preferably interacts with ligands having soft aromatic nitrogen and thiol donors [43,44]. The ^{99m}Tc-labeled complex was stable in vitro and in vivo in murine carcinoma S180 cells with no noticeable decomposition was observed even up to 24 h. The radiopharmaceutical (^{99m}Tc-2-MBI) has significantly high renal clearance and observed to be in consistent with other ^{99m}Tc-labeled renal agents including ^{99m}Tc-MAG3, ^{99m}TcMAEC and ^{99m}Tc-EC [32]. It has been observed that ^{99m}Tc-2-MBI has high uptake in S180 tumor bearing mice as well as tumor/muscle and tumor/blood ratio were also found to be more challenging than other ^{99m}Tc-labeled imidazole based radiotracers reported in the literature [20,21]. As per concern for the uptake of radiotracer in non-targeted tissues and organs such as lungs, liver and intestine, our proposed radiotracer seems to be much superior than others at 4 h post-injection [45,46]. To the best of our knowledge and outcomes obtained from biological evaluation, this radiotracer can be significantly use as a potential radiotracer for detection of tumor hypoxia.

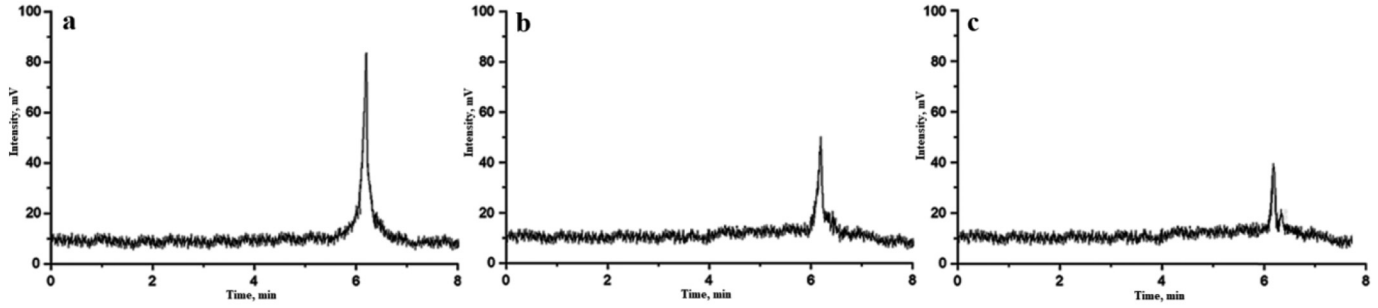

Fig. 7. Metabolic stability analysis carried out by radio-HPLC showing chromatograms (a) Urine (b) Blood and (c) Liver.

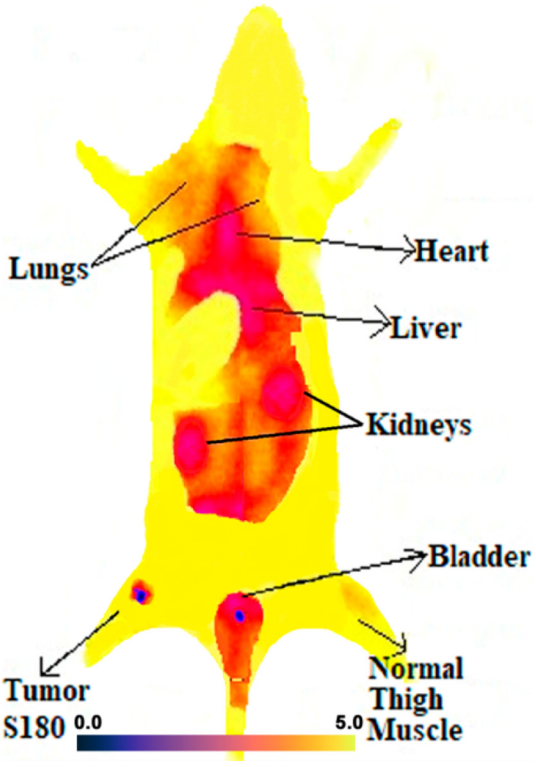

Fig. 8. Scintigraphic imaging study of ^{99m}Tc-2-MBI in S180 tumor induced Balb/c mice model indicating high uptake in tumor site as compare to normal muscle. The experiment was repeated thrice ($n = 3$).

Conclusion

In this study, ^{99m}Tc-$(CO)_3(H_2O)$-$C_7H_4N_2S$ (or ^{99m}Tc-2-MBI) complex was successfully synthesized with high radiochemical purity. The ^{99m}Tc-2-MBI holds neutral nature and good in vitro stability in saline and mice serum. In vivo biological evaluation results in mice bearing S180 tumor showed high selectivity and efficiency to accumulate in tumor tissue than normal muscle tissue. The biodistribution and scintigraphy imaging studies indicated that this radiopharmaceutical had evident tumor uptake and profound target/non-target ratio (T/B, T/M), suggesting ^{99m}Tc-2-MBI could be a potential radiotracer for early stage diagnosis of hypoxic tumor.

CRediT authorship contribution statement

Syed Faheem Askari Rizvi: Conceptualization, Methodology, Validation, Investigation, Writing - Original Draft. Haixia Zhang: Validation, Resources, Writing - Review & Editing, Supervision. Sajid Mehmood: Resources, Project administration. Mahmoud Sanad: Formal analysis, Visualization.

Acknowledgement

The authors are highly thankful to Dr. Muhammad Daud (Deputy Chief Scientist), Chemistry Division for providing all necessary facilities of radiation use and animal studies, and Dr. Fuming Zhang for providing analytical techniques facility for characterizations.

Funding

This research did not receive any specific grant from funding agencies in the public, commercial, or not-for-profit sectors.

Declaration of competing interest

The authors declare no potential conflict of interest.

Appendix A. Supplementary data

Supplementary data to this article can be found online at https://doi.org/10.1016/j.tranon.2020.100854.

References

[1] C. Ràfols, E. Bosch, R. Ruiz, K.J. Box, M. Reis, C. Ventura, S. Santos, M.E. Araújo, F. Martins, Acidity and hydrophobicity of several new potential antitubercular drugs: isoniazid and benzimidazole derivatives, J. Chem. Eng. Data 57 (2) (2012) 330–338.
[2] Y.-F. Li, G.-F. Wang, P.-L. He, W.-G. Huang, F.-H. Zhu, H.-Y. Gao, W. Tang, Y. Luo, C.-L. Feng, L.-P. Shi, Y.-D. Ren, W. Lu, J.-P. Zuo, Synthesis and anti-hepatitis B virus activity of novel benzimidazole derivatives, J. Med. Chem. 49 (15) (2006) 4790–4794.
[3] Y.-B. Bai, A.-L. Zhang, J.-J. Tang, J.-M. Gao, Synthesis and antifungal activity of 2-chloromethyl-1H-benzimidazole derivatives against Phytopathogenic Fungi in vitro, J. Agric. Food Chem. 61 (11) (2013) 2789–2795.
[4] Shaharyar M. Salahuddin, A. Mazumder, Benzimidazoles: a biologically active compounds, Arab. J. Chem. 10 (01) (2017) (S157-S73).
[5] A. Subramaniyan, P.K. Helen, S. Samiyappan, A. Rajaram, Biologically Active Benzimidazole Derivatives, Mini-Reviews in Organic Chemistry. 12 (2) (2015) 178–195.
[6] M.F. AlAjmi, A. Hussain, M.T. Rehman, A.A. Khan, P.A. Shaikh, R.A. Khan, Design, synthesis, and biological evaluation of benzimidazole-derived biocompatible copper(II) and zinc(II) complexes as anticancer chemotherapeutics, Int. J. Mol. Sci. 19 (5) (2018) 1492–1514.
[7] F.A. Tanious, D. Hamelberg, C. Bailly, A. Czarny, D.W. Boykin, W.D. Wilson, DNA sequence dependent monomer – dimer binding modulation of asymmetric benzimidazole derivatives, J. Am. Chem. Soc. 126 (1) (2004) 143–153.
[8] G. Mariappan, R. Hazarika, F. Alam, R. Karki, U. Patangia, S. Nath, Synthesis and biological evaluation of 2-substituted benzimidazole derivatives, Arab. J. Chem. 8 (5) (2015) 715–719.
[9] A.R. Katritzky, D. Jishkariani, R. Sakhuja, C.D. Hall, P.J. Steel, Carbene-mediated transformations of 1-(benzylideneamino)benzimidazoles, The Journal of Organic Chemistry. 76 (10) (2011) 4082–4087.
[10] N.N. Al-Mohammed, Y. Alias, Z. Abdullah, R.M. Shakir, E.M. Taha, A.A. Hamid, Synthesis and antibacterial evaluation of some novel imidazole and benzimidazole sulfonamides, Molecules. 18 (10) (2013) 11978–11995.
[11] M.T. Huynh, S.J. Mora, M. Villalba, M.E. Tejeda-Ferrari, P.A. Liddell, B.R. Cherry, A.-L. Teillout, C.W. Machan, C.P. Kubiak, D. Gust, T.A. Moore, S. Hammes-Schiffer, A.L. Moore, Concerted one-electron two-proton transfer processes in models inspired by the Tyr-His couple of photosystem II, ACS Central Science. 3 (5) (2017) 372–380.
[12] C. Raynaud, W. Daher, M.D. Johansen, F. Roquet-Banères, M. Blaise, O.K. Onajole, A.P. Kozikowski, J.-L. Herrmann, J. Dziadek, K. Gobis, L. Kremer, Active benzimidazole derivatives targeting the MmpL3 transporter in Mycobacterium abscessus, ACS Infectious Diseases. 6 (2) (2020) 324–337.
[13] T. de la Fuente, M. Martín-Fontecha, J. Sallander, B. Benhamú, M. Campillo, R.A. Medina, L.P. Pellissier, S. Claeysen, A. Dumuis, L. Pardo, M.L. López-Rodríguez, Benzimidazole derivatives as new serotonin 5-HT6 receptor antagonists. Molecular mechanisms of receptor inactivation, J. Med. Chem. 53 (3) (2010) 1357–1369.
[14] M.K. Kim, H. Shin, Park K-s, H. Kim, J. Park, K. Kim, J. Nam, H. Choo, Y. Chong, Benzimidazole derivatives as potent JAK1-selective inhibitors, J. Med. Chem. 58 (18) (2015) 7596–7602.
[15] G. Yuan, H. Liu, J. Gao, K. Yang, Q. Niu, H. Mao, X. Wang, X. Lv, Copper-catalyzed domino addition/double cyclization: an approach to polycyclic Benzimidazole derivatives, The Journal of Organic Chemistry. 79 (4) (2014) 1749–1757.
[16] M. Hranjec, K. Starčević, S.K. Pavelić, P. Lučin, K. Pavelić, G. Karminski Zamola, Synthesis, spectroscopic characterization and antiproliferative evaluation in vitro of novel Schiff bases related to benzimidazoles, Eur. J. Med. Chem. 46 (6) (2011) 2274–2279.
[17] S.M. Sondhi, R. Rani, J. Singh, P. Roy, S.K. Agrawal, A.K. Saxena, Solvent free synthesis, anti-inflammatory and anticancer activity evaluation of tricyclic and tetracyclic benzimidazole derivatives, Bioorg. Med. Chem. Lett. 20 (7) (2010) 2306–2310.
[18] Y. Zhang, T. Chu, X. Gao, X. Liu, Z. Yang, Z. Guo, X. Wang, Synthesis and preliminary biological evaluation of the 99mTc labeled nitrobenzoimidazole and nitrotriazole as tumor hypoxia markers, Bioorg. Med. Chem. Lett. 16 (7) (2006) 1831–1833.
[19] R. Alberto, New Organometallic Technetium Complexes for Radiopharmaceutical Imaging. Contrast Agents III: Radiopharmaceuticals – from Diagnostics to Therapeutics. Berlin, Heidelberg: Springer, Berlin Heidelberg 252 (2005) 1–44.
[20] Z. Li, J. Zhang, Z. Jin, W. Zhang, Y. Zhang, Synthesis and biodistribution of novel 99mTc labeled 4-nitroimidazole dithiocarbamate complexes as potential agents to target tumor hypoxia, MedChemComm. 6 (6) (2015) 1143–1148.
[21] Q. Ruan, X. Zhang, X. Lin, X. Duan, J. Zhang, Novel 99mTc labelled complexes with 2-nitroimidazole isocyanide: design, synthesis and evaluation as potential tumor hypoxia imaging agents, MedChemComm. 9 (6) (2018) 988–994.
[22] R.B.P. Elmes, Bioreductive fluorescent imaging agents: applications to tumour hypoxia, Chem. Commun. 52 (58) (2016) 8935–8956.
[23] I. Ali, M.N. Lone, H.Y. Aboul-Enein, Imidazoles as potential anticancer agents, MedChemComm. 8 (9) (2017) 1742–1773.
[24] Z. Wang, X. Deng, R. Xiong, S. Xiong, J. Liu, X. Cao, X. Lei, Y. Chen, X. Zheng, G. Tang, Design, synthesis and biological evaluation of 3′,4′,5′-trimethoxy flavonoid benzimidazole derivatives as potential anti-tumor agents, MedChemComm. 9 (2) (2018) 305–315.
[25] A. Sharma, J.F. Arambula, S. Koo, R. Kumar, H. Singh, J.L. Sessler, J.S. Kim, Hypoxia-targeted drug delivery, Chem. Soc. Rev. 48 (3) (2019) 771–813.

[26] I.N. Fleming, R. Manavaki, P.J. Blower, C. West, K.J. Williams, A.L. Harris, J. Domarkas, S. Lord, C. Baldry, F.J. Gilbert, Imaging tumour hypoxia with positron emission tomography, Br. J. Cancer 112 (2) (2015) 238–250.
[27] K.A. Krohn, J.M. Link, R.P. Mason, Molecular imaging of hypoxia, J. Nucl. Med. 49 (02) (2008) (129S-48S).
[28] G. Mees, R. Dierckx, C. Vangestel, C. Van de Wiele, Molecular imaging of hypoxia with radiolabelled agents, Eur. J. Nucl. Med. Mol. Imaging 36 (10) (2009) 1674–1686.
[29] L.J. Dubois, R. Niemans, S.J.A. van Kuijk, K.M. Panth, N.-K. Parvathaneni, S.G.J.A. Peeters, C.M.L. Zegers, N.H. Rekers, M.W. van Gisbergen, R. Biemans, et al., New ways to image and target tumour hypoxia and its molecular responses, Radiother. Oncol. 116 (3) (2015) 352–357.
[30] R. Alberto, R. Schibli, A. Egli, A.P. Schubiger, U. Abram, T.A. Kaden, A novel organometallic aqua complex of technetium for the labeling of biomolecules: synthesis of [99mTc(OH2)3(CO)3]+ from [99mTcO4]- in aqueous solution and its reaction with a bifunctional ligand, J. Am. Chem. Soc. 120 (31) (1998) 7987–7988.
[31] H.C. Kolb, M.G. Finn, K.B. Sharpless, Click chemistry: diverse chemical function from a few good reactions, Angew. Chem. Int. Ed. 40 (11) (2001) 2004–2021.
[32] M. Lipowska, H. He, E. Malveaux, X. Xu, L.G. Marzilli, A. Taylor, First evaluation of a 99mTc-tricarbonyl complex, 99mTc(CO)3(LAN), as a new renal radiopharmaceutical in humans, J. Nucl. Med. 47 (6) (2006) 1032–1040.
[33] I.K. Jebur, S. Mohammed Ismail, Synthesis, characterazition of some 2-mercapto-5-methoxy-1H-benzimidazole and test with some plant pathogenic fungi, J. Phys. Conf. Ser. 1294 (05) (2019) (052-34).
[34] A.O. Gezerman, B. Çorbacıoğlu, 2-Mercaptobenzimidazole, 2-mercaptobenzothiazole, and thioglycolic acid in an electroless nickel-plating Bath, E-Journal of Chemistry. 2015 (02) (2015) 1–11.
[35] F.S. Murakami, K.L. Lang, C. Mendes, A.P. Cruz, M.A. Carvalho Filho, M.A. Silva, Physico-chemical solid-state characterization of omeprazole sodium: thermal, spectroscopic and crystallinity studies, J. Pharm. Biomed. Anal. 49 (1) (2009) 72–80.
[36] X. Song, Q. Gan, X. Zhang, J. Zhang, Synthesis and biological evaluation of novel 99mTc-labeled palbociclib derivatives targeting cyclin-dependent kinase 4/6 (CDK4/6) as potential cancer imaging agents, Mol. Pharm. 16 (10) (2019) 4213–4222.
[37] S.F.A. Rizvi, S. Tariq, M. Mehdi, A.J. Hassan, Synthesis of 99mTc-roxithromycin: a novel diagnostic agent to discriminate between septic and aseptic inflammation, Chem. Biol. Drug Des. 93 (06) (2019) 1166–1174.
[38] N. Vijayan, R. Ramesh Babu, R. Gopalakrishnan, P. Ramasamy, W.T.A. Harrison, Growth and characterization of benzimidazole single crystals: a nonlinear optical material, J. Cryst. Growth 262 (01) (2004) 490–498.
[39] N. Vijayan, K. Nagarajan, A.M.Z. Slawin, C.K. Shashidharan Nair, G. Bhagavannarayana, Growth of benzimidazole single crystal by Sankaranarayanan−Ramasamy method and its characterization by high-resolution X-ray diffraction, thermogravimetric/differential thermal analysis, and birefringence studies, Cryst. Growth Des. 7 (2) (2007) 445–448.
[40] M. Höckel, P. Vaupel, Tumor hypoxia: definitions and current clinical, biologic, and molecular aspects, Journal of the National Cancer Institute. 93 (4) (2001) 266–276.
[41] W. Mueller-Klieser, K.H. Schlenger, S. Walenta, M. Gross, U. Karbach, M. Hoeckel, P. Vaupel, Pathophysiological approaches to identifying tumor hypoxia in patients, Radiother. Oncol. 20 (01) (1991) 21–28.
[42] J.D. Chapman, Measurement of tumor hypoxia by invasive and non-invasive procedures: a review of recent clinical studies, Radiother. Oncol. 20 (01) (1991) 13–19.
[43] H.J. Pietzsch, A. Gupta, M. Reisgys, A. Drews, S. Seifert, R. Syhre, H. Spies, R. Alberto, U. Abram, P.A. Schubiger, B. Johannsen, Chemical and biological characterization of technetium(I) and rhenium(I) tricarbonyl complexes with dithioether ligands serving as linkers for coupling the Tc(CO)3 and Re(CO)3 moieties to biologically active molecules, Bioconjug. Chem. 11 (03) (2000) 414–424.
[44] S. Alves, A. Paulo, J.D.G. Correia, Â. Domingos, I. Santos, Coordination capabilities of pyrazolyl containing ligands towards the fac-[Re(CO)3]+ moiety, J. Chem. Soc. Dalton Trans. 2002 (24) (2002) 4714–4719.
[45] T. Chu, S. Hu, B. Wei, Y. Wang, X. Liu, X. Wang, Synthesis and biological results of the technetium-99m-labeled 4-nitroimidazole for imaging tumor hypoxia, Bioorg. Med. Chem. Lett. 14 (3) (2004) 747–749.
[46] K. Vats, M.B. Mallia, A. Mathur, H.D. Sarma, S. Banerjee, '4+1' mixed ligand strategy for the preparation of 99mTc-radiopharmaceuticals for hypoxia detecting applications, ChemistrySelect. 2 (10) (2017) 2910–2916.